# PERFORMANCE OF THE D0 END CALORIMETER ELECTROMAGNETIC MODULE<sup>1</sup>

Hiroaki Aihara

Lawrence Berkeley Laboratory University of California Berkeley, CA 94720

October 1990

DISTRIBUTION OF THIS DOCUMENT IS UNLIMITED

<sup>&</sup>lt;sup>1</sup>This work was supported by the Director, Office of Energy Research, Office of High Energy and Nuclear Physics, Division of High Energy Physics, of the U.S. Department of Energy under Contract No. DE-AC03-76SF00098.

# Performance of the D0 End Calorimeter Electromagnetic Module\*

Hiroaki Aihara Lawrence Berkeley Laboratory, University of California, Berkeley, California 94720 (Representing the D0 collaboration<sup>†</sup>)

presented at 1990 IEEE Nuclear Science symposium, Arlington, Virginia, October 23-26, 1990

### Abstract

We have constructed a Uranium liquid Argon calorimeter which serves as the end calorimeter electromagnetic modale for the D0 experiment at Fermilab. We present details of the construction and the results of the tests made using electron beams ranging from 10 GeV to 150 GeV. We find the energy resolution is  $15.5\%/\sqrt{E(GeV)}$  with a small constant term of  $\sim 0.5\%$  and the response is linear to better than  $\pm 0.5\%$ .

### 1 Introduction

D0 is an experiment presently under construction for the Fermilab Tevatron collider. The detector is in the final stage of the assembly and will begin taking data in mid-1991. The detector features fine-grained Uranium liquid Argon calorimeter modules which provide good energy resolution and hermetic coverage for electrons, photons and jets. The calorimeter system consists of three separate cryostats, central (CC) and ends (EC), each of which contains electromagnetic and hadronic calorimeter modules. Figure 1 shows the layout of central and end calorimeters.

We have operated a test beam facility at Fermilab in order to test and calibrate the various calorimeter modules. In a 1987-88 run[1] we tested full prototypes of two calorimeter modules, central electromagnetic(CCEM) and end middle hadronic (ECMH) modules, and confirmed

**ECOH** 

**ECMH** 

**ECIH** 

**CCCH** 

**CCFH** 

CCEM

Central

Detectors

netic (ECEM) and inner hadronic (ECIH) modules.

The goal of this test was to measure the performance and calibrate the final modules with electrons and pions, prior to the installation in the D0 cryostat. In this article we present the results from this test of the ECEM module.

### \*This work was supported by the Director, Office of Energy Research of the U.S. Department energy under Contract No.DE-AC03-

### Construction of the module

The ECEM module provides full azimuthal (4) coverage in the forward region  $(1.4 < \eta < 4.0)^{\ddagger}$ . The basic sampling cell of the module consists of a 4 mm depleted Ucanium

Figure 1: Layout of the Calorimeters. Only one half of the calorimeter system is shown. their capability to perform to design specifications. During the period between June and August 1990 we made tests on two final modules of the end calorimeter, electromag-

<sup>&</sup>lt;sup>†</sup> D0 collaboration includes members from University of Arizona. Brookhaven National Laboratory, Brown University, University of California Riverside, Columbia University, Fermi National Accelerator Laboratory, Florida State University, University of Florida, University of Hawaii, Indiana University, Lawrence Berkeley Laboratory, University of Maryland, University of Michigan, Michigan State University, New York University, Northern Illinois University, Northwestern University, University of Rochester, CEN Saclay France, Institute for High Energy Physics Serpukhov USSR, State University of New York - Stony Brook, Tata Institute of Fundamental Research Bombay India, Texas A&M University and Yale University.

 $<sup>^{4}\</sup>eta$  is the psedorapidity defined as  $\eta = -ln \tan(\theta/2)$ , where  $\theta$  is the polar angle from the beam axis.

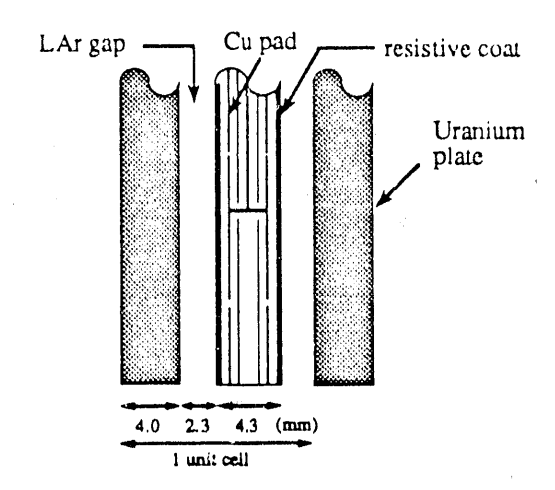


Figure 2: The basic sampling cell of the ECEM, showing Uranium plates, liquid Argon gaps and a multilayer PC signal board.

absorber plate, a 2.3 mm liquid Argon gap, a NEMA G-10 signal board and another 2.3 mm liquid Argon gap, as is shown in Fig.2. The module contains about 20 radiation lengths ( $X_0$ ) of material in 18 cells. The module is read out in four separate longitudinal sections of 0.3, 2.6, 7.9 and 9.3  $X_0$ . Transverse segmentation is provided by the readout pads on the signal boards, each covering an  $\eta$ ,  $\phi$  interval of  $\Delta \eta \times \Delta \phi = 0.1 \times \pi/32 (\approx 0.1)$ . In the third longitudinal section, which typically contains 65% of the electromagnetic shower, the transverse segmentation is doubled in both directions (0.05 × 0.05) to determine the position of the shower. These pads are arranged to make a semi-projective tower geometry.

Figure 3 shows the cross section of the ECEM. Both absorbers and signal boards are disks with a typical outer radius of 1 m. The first two absorber disks are thin (1.5) mm) stainless steel disks to form massless gaps to monitor the energy flow through the cryostat wall which has a total of about 2X<sub>0</sub>. Each Uranium disk is made by joining 3 smaller plates side by side at their edges. The thickness of each disk was measured and the variation in thickness was ~ 2.3% and ~ 1% in Uranium disks and signal disks, respectively. All absorber and signal disks are supported from a 2 cm thick stainless steel strongback in the middle of the module by an aluminum central tube and titanium tie rods. The tie rods also serve to flatten the Uranium plates. Platinum resistor temperature devices (RTDs) are attached to the module to monitor the thermal stress during cooldown and warmup.

A signal disk consists of sixteen 22.5° wedge shaped printed circuit (PC) boards laminated with NEMA G-10 face sheets coated with high resistivity ( $\sim 50 \text{M}\Omega/\Box$ ) epoxy. Each PC board is a 5-layer board with copper pads on the outer surfaces and signal traces on the inner layer which bring the signals to the connectors mounted at the perimeter of the disk. Two shielding ground planes reduce crosstalk to a negligible level. The cross section of a PC

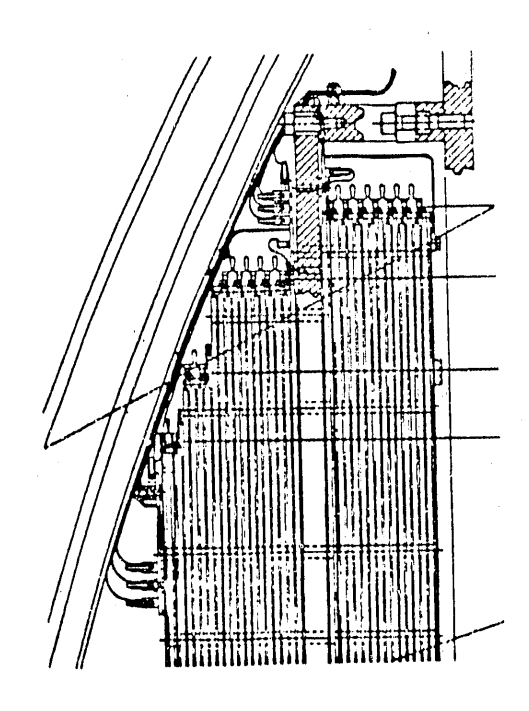


Figure 3: Cross section of the ECEM. Only a portion of the ECEM is shown.

board is shown in Fig.2.

Positive high voltage is applied to the resistive coat on the face sheets. Ground connections to the Uranium plates were made using welded Niobium pins. The normal operating voltage is +2.5 kV, corresponding to a drift field of 1.1 kV/mm in the gap.

The module has 7488 readout channels. Low impedance  $(30\Omega)$  coaxial cables are used within the cryostat to carry signals to the multilayer feedthrough boards which reorder the signals so that all the signals in a particular tower become adjacent. The outputs from the charge-sensitive preamplifiers mounted on the cryostat are connected to the shaping and sampling hybrids circuits by twisted pair cables. The shaped signals are sampled twice with an interval of 2.5 µs for baseline subtraction. The resulting signals are multiplexed (16 signals to 1 line) and double-buffered to reduce dead time, and fed to the ADCs through ×1/×8 switchable amplifiers which provide 15-bit equivalent dynamic range with a 12-bit ADC. The ADCs reside in a VME crate and a backplane VME bus is used to read the ADC outputs into a VME buffer, which in turn sends the data to the dual-port memories of a set of Micro VAX-Il computers. One ADC crate digitizes 4608 calorimeter signals in approximately 160  $\mu s[2]$ .

## 3 Test beam setup

The test beam facility has been built in the Neutrino-West beam line at Fermilab. Triggering was provided by a set of scintillation counters. A system of proportional wire chambers (PWCs) and Cherenkov counters provided the

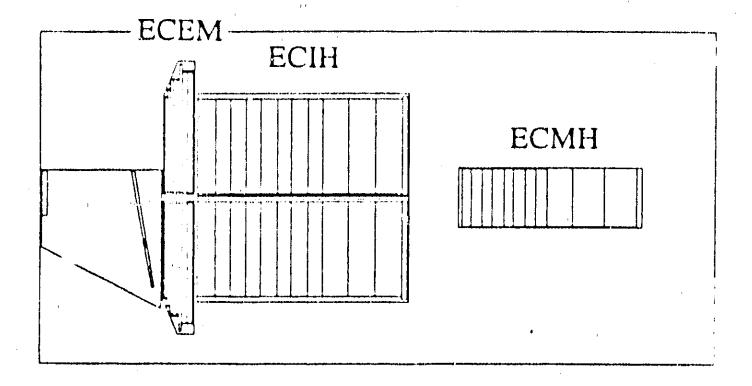


Figure 4: Arrangement of modules in the test beam cryostat. A liquid Argon excluder, ECEM, ECIII and ECMII are shown.

particle momentum and identification on an event-by-event basis. The spread of the beam momentum was typically 1.5% and the pion contamination in the electron beam was negligible (less than  $10^{-5}$ ). Arrangement of modules in the test beam cryostat is shown in Fig.4. An ECMH module was placed behind the ECIH to monitor the leakage of hadronic showers. The cryostat has a thin window for the region illuminated by the beam. The setup includes a liquid Argon excluder, a 4.4 cm thick aluminum plate and a 2.5 cm thick stainless steel plate to simulate the material in front of the ECEM in the final D0 detector. The test beam cryostat is equipped with a transporter so that the beam can sweep the module over  $\pm 15$  degrees in  $\phi$  and the full  $\eta$  extent.

The region illuminated by the beam was instrumented with the readout electronics which will be used in the final D0 detector. The electronics was periodically (typically once a day) calibrated with a precision pulser which injects charge into each preamplifier channel. The channel-to-channel variation in gain was found to be  $\sim 2.6\%$  (rms). The intrinsic noise of the electronics was measured to be [3]  $\sigma_{elect} = (2000 + 3100 \times C_d(nF))$  electrons,  $C_d$  being the capacitance of the electronic channel. The overall sensitivity [2] of the electronics is  $\sim 0.57$  fC per ADC count or 3600 electrons per count. One ADC count also corresponds to  $\sim 4$  MeV of electromagnetic energy deposited in the ECEM.

## 4 Data analysis

ADC pedestals and gains were corrected for each channel based on pulser calibration data. The spread in the beam momentum was corrected event-by-event using the momentum measured by the PWC system. Electrons which showered in the upstream material in the beam line were removed offline using the information from a PWC mounted on the face of the cryostat.

The energy of the electromagnetic shower was reconstructed by summing all 4 longitudinal sections  $(20X_0)$  in

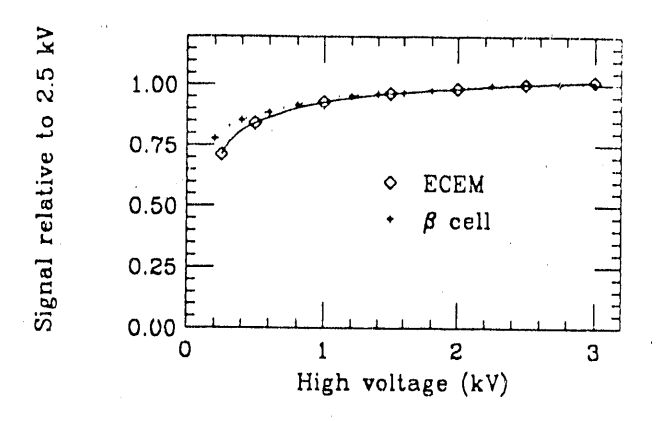


Figure 5: High voltage plateau curve of the ECEM taken with 100 GeV electrons. Also shown is the plateau curve of the liquid Argon purity monitor ( $\beta$  cell). The curves are normalized to unity at 2.5 kV

the ECEM and the first section  $(30X_0)$  of the ECIH. The signal in each longitudinal section was calculated by dividing the number of ADC counts by the effective sampling fraction (the energy in the liquid Argon gap divided by the total energy in a sampling cell). The effective sampling fractions were obtained by minimizing the width of the energy response of a separate set of data. These values are consistent with calculated sampling fractions. The analyses presented here used a single set of energy independent effective sampling fractions.

The results were obtained by adding together the energy in the  $\upsilon$  towers enclosing the shower maximum. We found  $\sim 99\%$  of the incident energy was contained in these towers. The effect of variation in thickness of the Uranium plates and signal boards was corrected tower-by-tower by using thickness maps obtained during the construction.

### 5 Performance

### 5.1 High voltage plateau

Figure 5 shows the high voltage plateau curve obtained with 100 GeV electrons. Our operating voltage (2.5kV) is well within the plateau. Also shown is the plateau curve of the liquid Argon purity monitor (3 cell§) which agrees well with the ECEM data. The purity of liquid Argon was maintained at  $\leq$  0.6 ppm oxygen-equivalent contamination over the entire period of data taking, and the response of the ECEM was stable to better than  $\pm 1\%$ .

### 5.2 Response as a function of energy

The pulse height distributions of electrons obtained according to the analysis described above are shown in Fig.6

 $<sup>{}^{6}\!\!\!/\</sup>beta$  cell is a double liquid Argon gap with Ru(106)  $\beta$  source. [4]

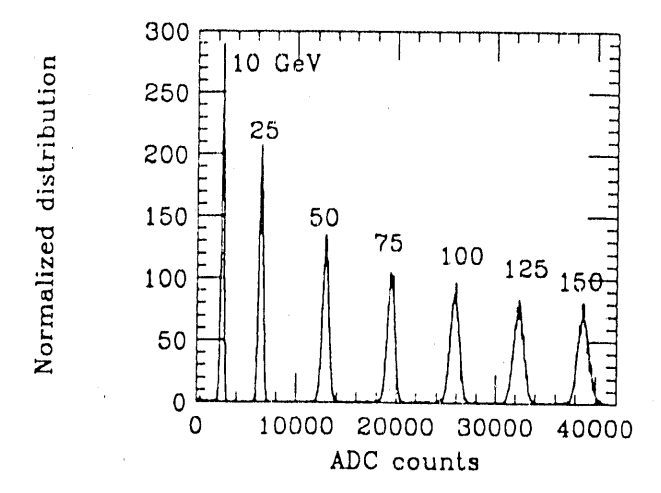


Figure 6: Pulse height distributions of electrons for 10, 25, 50, 75, 100, 125 and 150 GeV/c. Gaussian fits are superimposed. The distributions are normalized to the same number of events.

for beam momenta of 10, 25, 50, 75, 100, 125 and 150 GeV/c. All distributions are well represented by Gaussian functions and therefore the mean  $(\mu)$  and width  $(\sigma)$  were determined by the Gaussian fit. Figure 7 shows the mean pulse heights vs beam momenta with a straight line fit. Also shown is the deviation from the fitted straight line, defined as (data-fit)/fit. The deviation from linearity is less than  $\pm 0.5\%$  over the entire momentum range. The fit gives

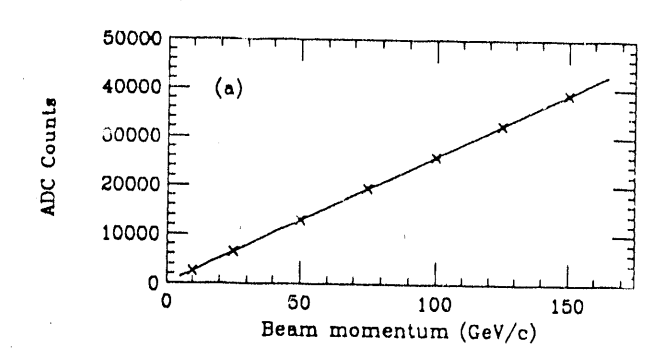
 $E(GeV) = \mu(ADCcounts)/(259.0\pm0.1) - 0.09\pm0.01(GeV)$ 

### 5.3 Energy resolution

The fractional resolution was calculated as  $\sigma/\mu$  from a Gaussian fit described in the previous section. We assume the energy dependence of the resolution is  $(\sigma/\mu)^2 = C^2 + S^2/E + N^2/E^2$ , where E is the beam energy in GeV, C is a constant contribution from systematic errors such as remaining channel-to-channel variation in gain, S is due to the statistical error in sampling, and N represents energy independent contributions to  $\sigma$  such as electronic and Uranium noise. Figure 8 shows the values of  $\sigma/\mu$  superimposed with the result of the fit. The results of the fit are:

$$C = 0.005 \pm 0.001,$$
  
 $S = 0.155 \pm 0.003(\sqrt{\text{GeV}}), \text{ and }$   
 $V = 0.226 \pm 0.023(\text{GeV}).$ 

The value of the noise term, N, agrees well with the directly measured value. The results are in good agreement with the specifications in the D0 design report[5] and the



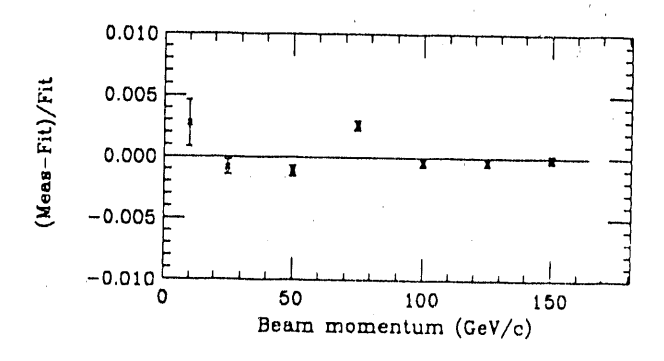


Figure 7: (a) The mean pulse heights vs beam momenta with a straight line fit superimposed. (b) Fractional differences between measured response and a straight line fit.

results reported in the previous test beam run[1].

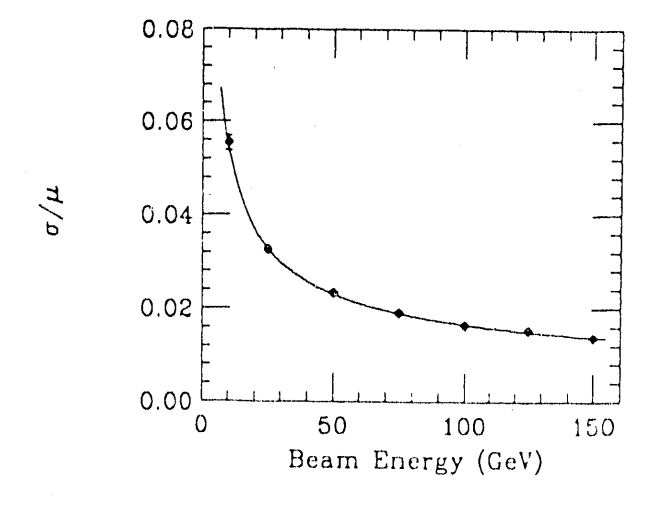


Figure 8: The fractional energy resolution  $\sigma/\mu$  as a function of electron beam energy superimposed with the fit described in the text.

### 6 Conclusion

The performance of the D0 end calorimeter electromagnetic module was tested using electrons with energy ranging from 10 to 150 GeV. The energy resolution is  $15.5\%/\sqrt{\mathrm{E}~(\mathrm{GeV})}$  with a small constant term of  $\sim 0.5\%$  and the response is linear to better than  $\pm 0.5\%$ .

We thank the Fermilab Accelerator Division and the staffs at our individual institutions for their exceptional performance. This work was supported by the Director, Office of Energy Research of the U.S. Department of Energy under Contract No. DE-AC03-76SF00098.

### References

- [1] M.Abolins et al., Nucl.Instr.and Meth.A280(1989)36.
- [2] P.Franzini, Nucl.Instr.and Meth.A289(1990)438.
- [3] R.D.Schamberger, Proceedings of the 2nd International Conference on Advanced Technology and Particle Physics, Como, Italy, 11-15 June, 1990.
- [4] G.C.Blazey, D0 internal note D0-940 (March 1990) unpublished.
- [5] D0 Design Report, The D0 collaboration (1984) unpublished.

# DATE FILMED OI108/191

.

H #

the second secon